To the Graduate Council:

I am submitting herewith a thesis written by William H. Zielke entitled "A Study of the Nitric Acid Corrosion Rate Results as Determined by ASTM A-262 Practice C on TP-304-L Tubular Products." I recommend that it be accepted in partial fulfillment of the requirements for the degree of Master of Science, with a major in Metallurgical Engineering.

E. E. Stansbury

Dr. E. E. Stansbury, Major Professor

We have read this thesis and recommend its acceptance:

C R Brooks

Accepted for the Council:

L Evans Roth

Vice Chancellor
Graduate Studies and Research

D

A STUDY OF THE NITRIC ACID CORROSION RATE RESULTS AS DETERMINED BY ASTM A-262 PRACTICE C ON TP-304-L TUBULAR PRODUCTS

A Thesis

Presented for the

Master of Science

Degree

The University of Tennessee, Knoxville

William H. Zielke

March 1979

ABSTRACT

Basic metallurgical factors affecting the corrosion behavior of wrought TP-304-L tubular products in the ASTM A-262 Practice C (Nitric Acid) corrosion test is reviewed. Over 100 heats of TP-304-L were selected statistically to provide a range of variables within ASTM tubular product specifications. Significant factors identified as affecting the corrosion rate were carbon, chromium, nickel, ferrite phase and molybdenum with the ferrite phase. Maintaining carbon and nickel concentrations constant small increases in the chromium content greatly influence the formation of ferrite. A small amount of residual ferrite--1 to 5%--significantly reduces the corrosion rate in nitric acid. However, residual ferrite in conjunction with molybdenum concentrations over 0.25% increases the corrosion rate.

TABLE OF CONTENTS

LIST OF TABLES

LIST OF FIGURES

CHAPTER I

INTRODUCTION

Low carbon austenitic stainless steels were first developed in the early 1930's[1,2] and produced to a 0.07% carbon limit. Although initial specifications required .08% or .10% maximum carbon contents as a means of preventing intergranular corrosion[1], the performance of stainless steels in the chemical industry provided a strong incentive to produce lower carbon content alloys. During the early 1940's an extrapolated 0.04% carbon content was theorized to be low enough to prevent intergranular corrosion. Laboratory induction furnace heats of 0.03% carbon content were produced at the Carnegie-Illinois Steel Corporation[3]. This was the beginning of the present ASTM maximum carbon content of 0.035% carbon concentration on the low carbon austenitic stainless steels for tubular products. During the mid 1940's small pilot plant heats were produced, followed by full scale production of thirty ton arc furnace heats of the low carbon austenitic stainless steel alloys.

Since these austenitic stainless steel alloys (see Table I) were developed to prevent intergranular corrosion, it became important to test or develop tests to determine the susceptibility of a particular heat to practical service conditions.

TABLE I

TYPICAL COMPOSITION OF AUSTENITIC STAINLESS STEEL ALLOYS

	Composition By Percent Weight							
Alloy	Ni	Cr	Mn	Si	C	Mo	Ti	Cb
304-L	10.0	18.5	1.6	.5	.02	.3	.01	.01
304	10.0	18.5	1.6	.5	.06	.3	.01	.01
316-L	14.0	16.5	1.6	.5	.02	2.3	.01	.01
316	13.0	16.5	1.6	.5	.06	2.3	.01	.01
321	10.0	18.5	1.6	.5	.06	.3	.35	.01
347	11.0	18.5	1.6	.5	.06	.3	.01	.65

The susceptibility of as-welded or improperly heat treated unstabilized austenitic stainless steels to intergranular corrosion was a severe problem, especially in the chemical industry. E. I. DuPont de Nemours and Company spearheaded the use of the new series of low carbon austenitic stainless steels. Through DuPont efforts the boiling 65 percent nitric acid test was adopted as a tentative recommended practice for testing for susceptibility to intergranular corrosion of stainless steels in 1944. It is significant to recognize that this test was intended to determine if a given lot of material was susceptible to intergranular corrosion--not to establish a corrosion rate for other media.

Although the establishment of the 0.035% carbon maximum greatly reduced the corrosion problem, work accomplished in the late 1940's established that a carbon content of 0.02% or less was more desirable to insure immunity from intergranular corrosion[1]. Rapid quenching from 1900°F or higher is the standard for the heat treatment of low carbon austenitic stainless steels[5]. This allows a maximum amount of carbon to go into solution at 1900°F and remain there by rapidly cooling.

CHAPTER II

PHYSICAL METALLURGY

The physical metallurgy of TP-304-L relevant to the boiling nitric acid test involves alloying elements, corrosion mechanism, heat treatment, sensitization phases present and grain size. To study the individual variables and relationships as many conditions as possible must be held constant.

A. Corrosion Mechanisms

Intergranular corrosion rates of austenitic stainless steels correlate with the amount of chromium carbide that is present in the grain boundary. The cause of this effect has been discussed over the last forty years[1-3,6-12]. When austenitic stainless steels are heat treated at 1950°F, chromium-bearing carbides dissolve to form a solution containing up to about 0.1% carbon. Rapid cooling from 1950°F to 1000°F minimizes the precipitation of these chromium carbides at the grain boundaries. Decreasing cooling rates results in chromium carbide precipitation also (see Figure 1).

Reheating the austenitic stainless steels to temperatures close to 1250°F can result in the precipitation of chromium carbides[1-3,6-12]. This precipitation is directly related to the carbon content, time and temperature--see Figure 2.

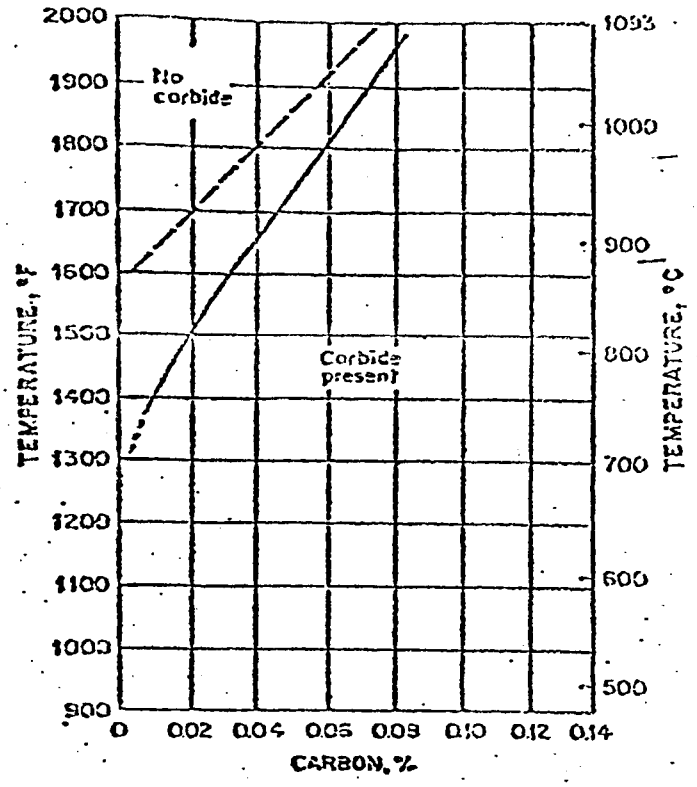

Figure 1. Solid solubility of carbon versus temperature.[12]

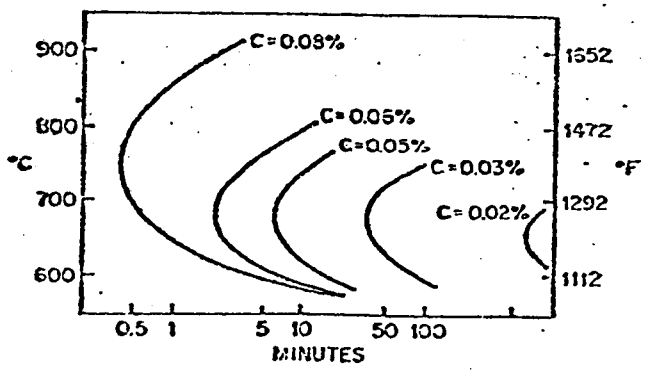

Figure 2. Time temperature sensitization diagram for five 18 Cr - 9 Ni steels with different carbon contents.[12]

Alloying elements affect this solubility as shown. For example, in Figure 3 below which indicates the effect of nickel.

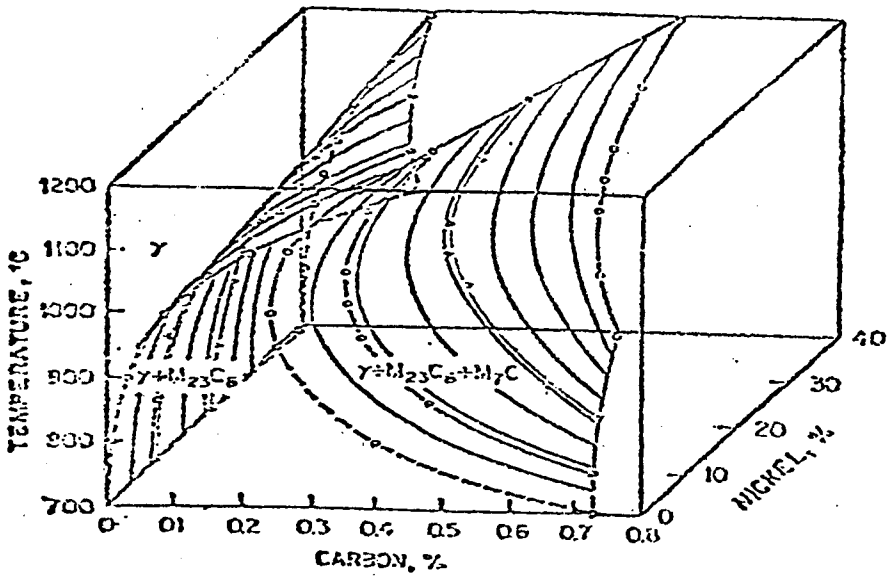

Figure 3. Solid solubility of carbon versus temperature with increasing nickel contents[12].

The normal time-temperature carbon concentration versus carbide precipitation causing response in Oxalic Acid Test is shown in Figure 1, previously referenced.

In addition to the fact that carbon promotes chromium carbide formation at the grain boundaries, it is also a strong austenite stabilizer. Both of these effects will be discussed in the results section of this paper.

The chromium depletion theory[9,10,12,13] attributes the intergranular attack of austenitic stainless steels to the precipitation of chromium carbides at the grain boundaries. When this occurs the depletion of chromium, in areas adjacent to the grain boundary, is below the concentration that is required for passivation in a given environment. This theory is based on the following four assumptions:

1. A chromium content of 12% is the minimum content required for a passive film.

2. The carbide precipitate at the grain boundary is predominately chromium carbide.

3. During heating to 1250°F the chromium in solution within the grains does not have time to diffuse back into the depleted grain boundary region.

4. The chromium depleted region has less than 12% chromium.

The strain related theory attributes intergranular attack to the distortion of the lattice close to the precipitate. The areas away from the carbide precipitates are unaffected by the strain. Thus, the attack occurs in the strained grain boundary areas.

The noble carbide theory contends that the intergranular corrosion is an electrochemical reaction between the carbide particles acting as cathodic surfaces supporting anodic dissolution of adjacent material. When a continuous path of carbides exist, the intergranular corrosion can proceed at a rapid pace[10].

These three theories led to research to more clearly define mechanism of intergranular attack of austenitic stainless steels. Microprobe analysis has shown that the chromium depleted region can have less than 12% chromium which supports the four assumptions of the chromium depletion theory; It has now become widely accepted. The strain related theory is discounted as the degree of strain is not sufficient to cause the severe attack[9]. The noble carbide theory has the problem that the potential of passive stainless steel has the same value as chromium carbide. However, where a chromium depleted area exists, electrochemical potentials could accelerate the corrosion rate.

Presently the chromium depletion mechanism aided by the noble carbide theory is the accepted mechanism for intergranular corrosion of austenitic stainless steels. In addition, the individual alloying elements and phases present contribute to the intergranular corrosion.

B. Heat Treatment and Sensitization

As previously pointed out, austenitic stainless steels are normally solution annealed at 1900°F or higher. The solid solubility of carbon is a function of temperature as shown in Figure 2, previously referenced. It is evident that, according to this diagram .06 to .07% carbon is soluble at 1900°F.

Rapid cooling to under 1000°F leaves up to .07% carbon in solid solution, but slow cooling between 1800°F and 1000°F results in carbide precipitation at the grain boundaries. Proper cooling, but reheating the steel between 1800°F and 1000°F, will also cause the carbides to precipitate. The resultant areas of lowered chromium content adjacent to the grain boundaries have lowered corrosion resistance and the material is described as being in a corrosion susceptible or "sensitized" condition.

C. Functions of Alloying Elements

The elements affecting the behavior of TP-304-L are carbon, manganese, phosphorus, sulfur, silicon, nickel, chromium, molybdenum and nitrogen. The ASTM Specification on composition is listed in Table II.

The austenite supersaturated with carbon following quenching is in an unstable condition. Therefore absolute immunity from chromium-carbide precipitation is almost, if not, impossible. Studies with 0.020% carbon TP-304-L have shown that if held in service for thousands of hours some chromium carbide will precipitate at 700-800°F relative to precipitation in hours near 1300°F.

Nickel contents over 9%, given that all other elements are held constant except iron, will increase the corrosion rate of TP-304-L[1,2,9,10,12]. The primary reason for this

TABLE II

TP-304-L CHEMISTRY COMPOSITION LIMITS[5]

Element	Composition Limits
Carbon	.035% Maximum
Manganese	2.00% Maximum
Phosphorus	.040% Maximum
Sulfur	.030% Maximum
Silicon	.75% Maximum
Nickel	8.00 to 13.0%
Chromium	18.0 to 20.0%
Nitrogen	Not Specified
Molybdenum	Not Specified

Only the chemistry ranges within this Specification are studied in this report

effect is that increasing the nickel content slightly decreases the solubility of carbon in the austenite (see Figure 3).

Chromium contents over the ASTM minimum specification of 18.0% have been reported to cause a slight decrease in the corrosion rates[1,2]. However, conflicting results can occur due to the formation of ferrite in the austenitic matrix with chromium concentrations of 19% to 20%. Chromium

concentrations of 18% are required for passivity of TP-304-L in most solutions.

Silicon introduces detrimental effects in contents over 1% in TP-304-L in the nitric acid test. TP-304-L is normally produced with a nominal silicon content of 0.5% and a maximum silicon content of 0.75%. Thus silicon has little detrimental effect on TP-304-L[9]. Silicon additions to extremely "pure," vacuum remelted, heats of TP-304-L have resulted in slightly worse nitric acid test results[8].

Molybdenum will slightly increase the corrosion rate of TP-304-L in the nitric acid test. It is a residual element introduced through scrap stainless steel, containing small amounts of molybdenum bearing stainless steels, used in melting heats of TP-304-L. Molybdenum is a ferrite former and concentrates in the ferrite phase if present.

Nitrogen has caused mixed effects in the nitric acid test depending on the concentration in TP-304-L[1]. Nitrogen is a very strong austenite former. Manganese is an austenite former and slightly increases the nitrogen solubility, but little is reported concerning the effect that manganese has on TP-304-L in the nitric acid test. Sulfur has a detrimental effect on the nitric acid test results of TP-304-L. Sulfides are slowly soluble in nitric acid, but due to the low levels of sulfur, below 0.030%, the total effect is small. Phosphorus has had no noticeable effect on the nitric acid corrosion rate with concentrations below 0.040%[1].

Grain size can have an effect on the corrosion rate of TP-304-L. Extremely large grains, grain size of 0, will generally reduce the corrosion rate in terms of weight loss due to the time required to cause a grain to be completely surrounded. Fine grained material, grain size of 10, will generally increase the corrosion rate. Most TP-304-L has a grain size of 5, due to final heat treatment of 1950°F followed by rapid cooling.

CHAPTER III

EXPERIMENTAL TECHNIQUE

The purpose of the ASTM A-262 Practice C Corrosion Test (Nitric Acid) is to detect susceptibility to intergranular corrosion[11]. Material which is susceptible in the nitric acid test may or may not be susceptible in a different corrosive media[10]. The nitric acid test will detect intergranular corrosion in TP-304-L due to carbide precipitation and hence grain boundary depletion of chromium.

A. Corrosion Test Procedure

The ASTM A-262 Practice C (Nitric Acid) Corrosion Test procedure consists of a test solution of 65$\pm$ 0.2 weight percent nitric acid[14]. The solution is prepared by mixing one liter of concentrated nitric acid (regent grade HNO_3, specific gravity 1.42) with 108 milliliters of distilled water.

The solution is placed in a one liter Ehrlenmeyer flask equipped with a 30 inch reflux condenser. A glass hook holds the sample in the boiling acid. Streicher has reported that this experimental technique is the most severe test apparatus for testing austenitic stainless steels[15]. All results listed in Appendix A were based on the use of this apparatus.

The samples were cut from tubular products with a slow

speed band saw and then ground with 120 grit paper exercising care to minimize the overheating of the sample. The specimens were then drilled and cleaned in acetone. The test consisted of five 48 hour test periods with a fresh solution of 65 weight percent nitric acid supplied after each test period. The extent of corrosion was measured by determining the loss of weight of the specimen after each test period. The corrosion rate is calculated from the following formula[14]:

$$\text{Inches per month} = \frac{WA}{dt}$$

W = Weight loss in grams (0.0000 grams)

A = Total surface area (0.000 cm^2)

d = Density (7.90 g/cm^3)

t = Time of exposure (hours)

The average of the five corrosion test results is used as the corrosion rate of the heat. The typical plot of the five test periods is listed in Figure 4.

B. Reproducibility

To reduce the number of variables, constraints were maintained on tube wall size, grain size and average test sample size. Duplicate samples were utilized initially to check these variables. Methods of quenching were also compared. These checks on the experimental technique were used to assure that observed variations in response to the

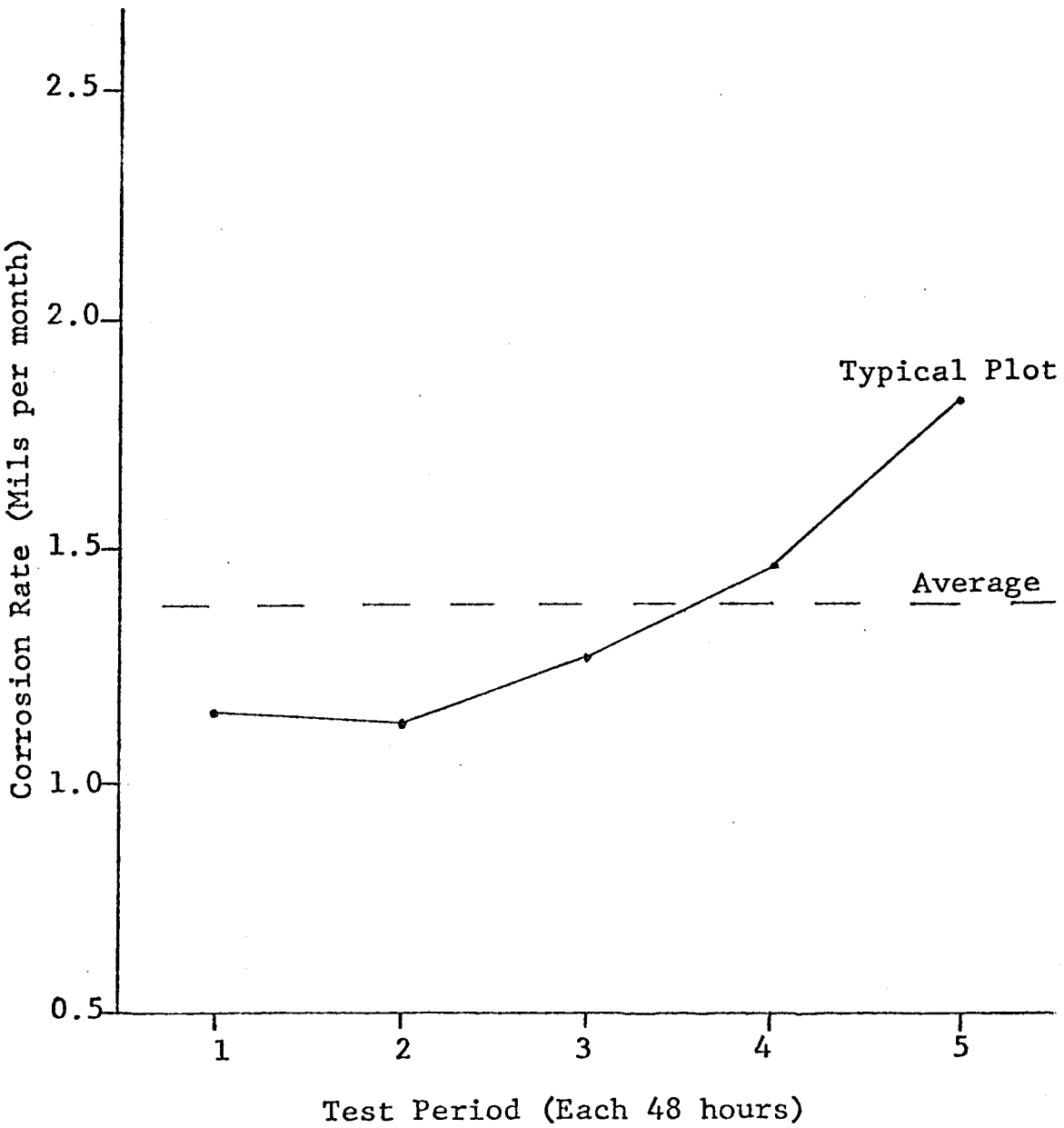

Figure 4. Typical plot of the five test periods of the Nitric Acid Test.

nitric acid test were true variations, not variations in test procedure, solution heat treatment or sample size.

The average size of the test samples was 3.0 in^2 and varied between 2.8 in^2 and 3.3 in^2. The average wall thickness of the test samples was 0.15 in and varied between 0.11 in and 0.22 in. The end grain effect varied between 18% and 30%; this is well below the ASTM A-262 Practice C recommended minimum of 50%[14].

The end grain effect is the apparent pitting of the material when viewed from the transverse cross section of a tubular product. During the processing of a tubular product most inclusions are greatly elongated in the longitudinal direction. These inclusions are preferentially attacked by the nitric acid solution. The pitting caused by the removal of these inclusions is maximized in the transverse cross section and is called end grain effect.

Duplicate samples were run on eight heats during the initial study and two additional heats later in the test group. The results are listed in Table III. The average difference was 0.12 mil per month. The three sigma variation was 0.27 mil per month. This is well within acceptable variation on the nitric acid test[16].

TABLE III

DUPLICATE NITRIC ACID TEST SAMPLES
(CORROSION RATE IN IPM)

Heat	1st Test	2nd Test	Difference
LWNN2N	.00129	.00138	.00009
LSM9F	.00086	.00084	.00002
LTE24A	.00187	.00184	.00003
LSM8D	.00109	.00076	.00025
LSM8A	.00075	.00074	.00001
XWMM5X	.00077	.00079	.00002
XWMN2T	.00190	.00174	.00016
XWNK23S	.00204	.00221	.00017
XWMN2S	.00155	.00137	.00018
LWNK23Z	.00180	.00158	.00022

D. Statistical Analysis Technique

Approximately 150 heats were selected for statistical analysis. These heats were selected from over 400 available heats having a range of compositions within the TP-304-L Specification. The concentrations of nine elements under study were individually averaged and these were selected as the "base" composition[17,18]. Heats were selected that had eight elements equal to the "base" composition and one element that varied from the "base" composition. See Table IV.

TABLE IV

TP-304-L BASE COMPOSITION WITH TEST VARIANCES

	Variation	Base Composition
Mn	1.2 to 1.8	1.6 ±0.1
Cr	18.0 to 19.4	18.5 ±0.3
Ni	9.4 to 11.0	10.0 ±0.2
Mo	.05 to .40	.10 ±0.05
Si	.35 to .65	.60 ±0.05
S	.009 to .020	.010 ±0.003
P	.012 to .023	.020 ±.005
C	.014 to .027	.020 ±.003
N	.022 to .061	.040 ±0.005

This method of sample selection restricted the range of composition of individual elements that could be studied. As a consequence, the effects of some of the elements were incompletely established due to the small range of compositions available.

E. Electrochemistry

The electrochemical aspects of the nitric acid test require consideration. Figure 5 shows the potential developed by the nitric acid test[10]. Superimposed on the potentiostatic curves for the compositions shown is the potential

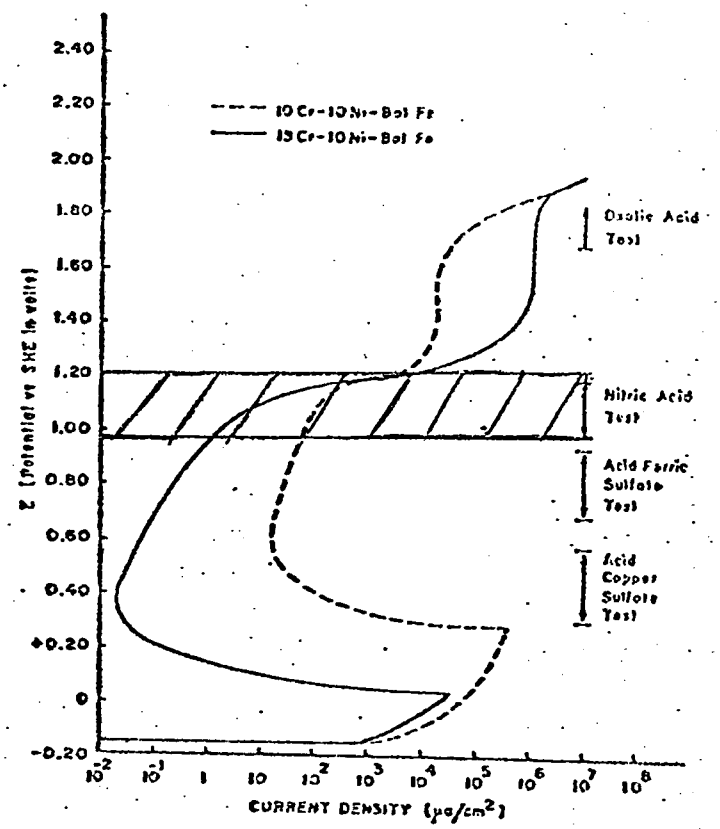

Figure 5. Schematic presentation of the range of corrosion potential expected from various corrosion tests[10].

range of the nitric acid test. The potential ranges for other media for ASTM A-262 are shown.

Figure 6 shows that the potential in the nitric acid test can vary from +1.0 to +1.2. In this same paper by Cowan and Tedmon[10], the effects of chromium content and sensitization time are considered. Although these curves

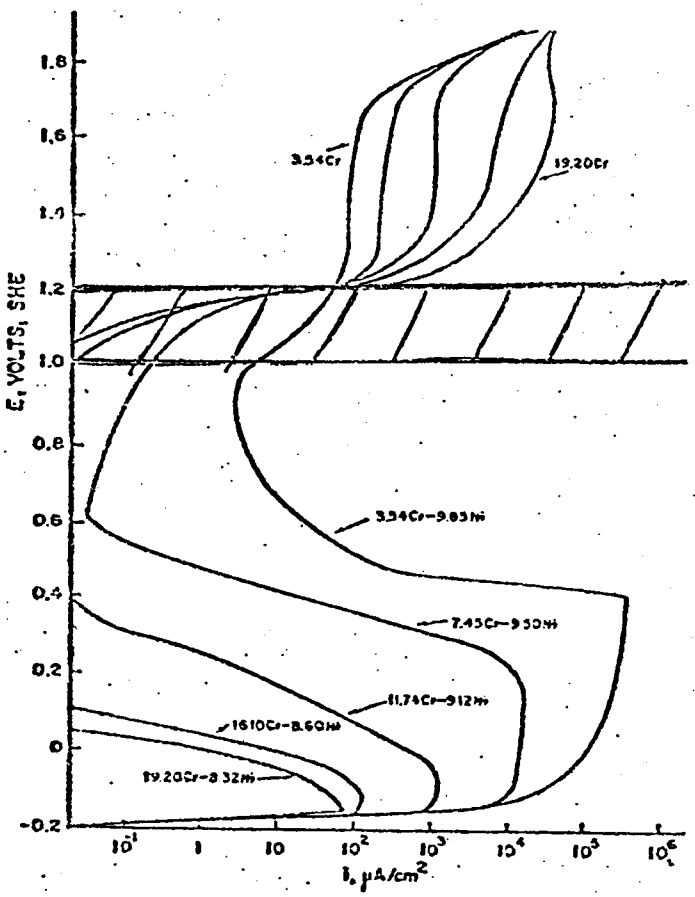

Figure 6. Anodic polarization curves of alloys of the iron - 9 nickel - balance chromium system in 1 N H_2SO_4.[10]

represent behavior in sulfuric acid, useful conclusions can be applied to the nitric acid test.

Figure 6 indicates that increasing the chromium content from 3.5% to 19.2% greatly decreases the current density and therefore decreases corrosion rate in the potential range of the nitric acid test. These polarization curves are for

homogoneous alloys, and clearly indicate the effect of increasing the chromium content.

The effect of sensitization time is shown in Figure 7 below.

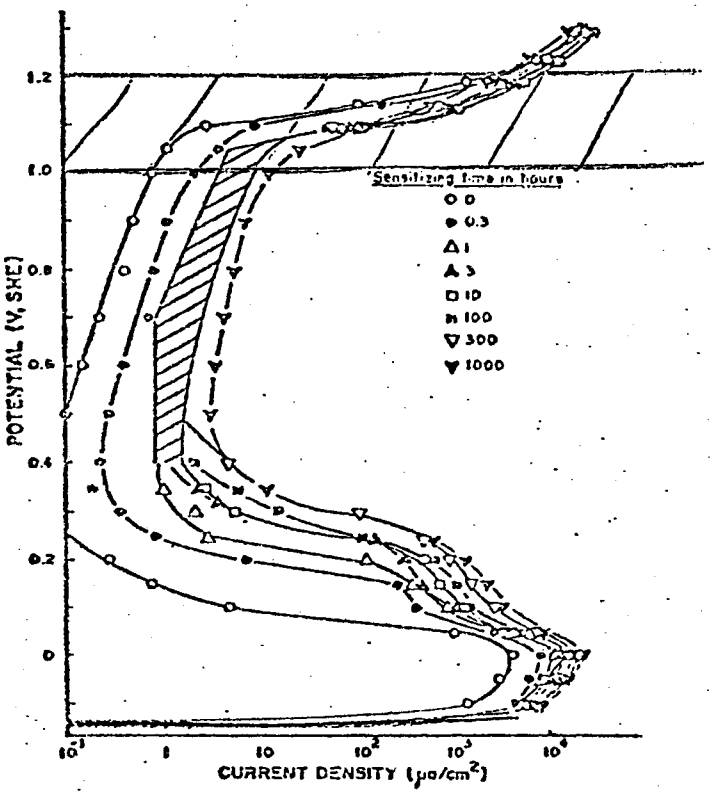

Figure 7. Effect of sensitization time on the steady-state anodic polarization curve of Type 304 Stainless Steel in 2N H_2SO_4 at 90°C.[10]

Increasing the sensitization time shifts the polarization curve to the right in sulfuric acid. Nitric acid test results would be expected to be similar. The increase in corrosion rate with longer sensitization times is consistent with the depletion of chromium in the austenitic grain boundaries due to the chromium carbide precipitate. The changes in corrosion rate can be large with sensitized materials. For example, at 1.1 volts, the current density increases from 1 a/cm^2 to 1000 a/cm^2. It is emphasized that these shifts result from localized decreases in chromium content near the grain boundaries. The function of the alloy which is depleted in chromium is relatively small when compared to the total surface area.

Two electro-potential tests were run. The results were 1.08 and 1.13 volts based on the standard hydrogen electrode. Both tests were mid range of the typical nitric acid test range of 1.0 to 1.2 volts.

CHAPTER IV

RESULTS AND DISCUSSION

A. Statistical Effects of Alloying Elements

Carbon content had the most significant effect on the corrosion rate, increasing proportionately with the carbon concentration in TP-304-L (see Figure 8). The carbon concentration varied from 0.014% to 0.027% with all other elements remaining constant. As the carbon concentration is increased over 0.025%, the corrosion rate increases greatly and approaches 2.0 mils per month. This rate is the maximum permitted by one large user of TP-304-L in nitric acid service. The results presented here correspond to traditional corrosion rates in nitric acid with increased carbon concentrations.

The nickel concentration had a slightly detrimental effect as the nickel concentration was increased from 9.5% to 10.5% (see Figure 9). This is consistent with the fact that the solubility of carbon is decreased with an increase of the nickel content. Figure 3, discussed on page 6, shows that this does occur. The lowered amount of carbon in solid solution will increase the corrosion rate. Although this effect was observed in this work, the small spread in nickel concentrations resulted in a minimal increase in corrosion rate in the nitric acid test.

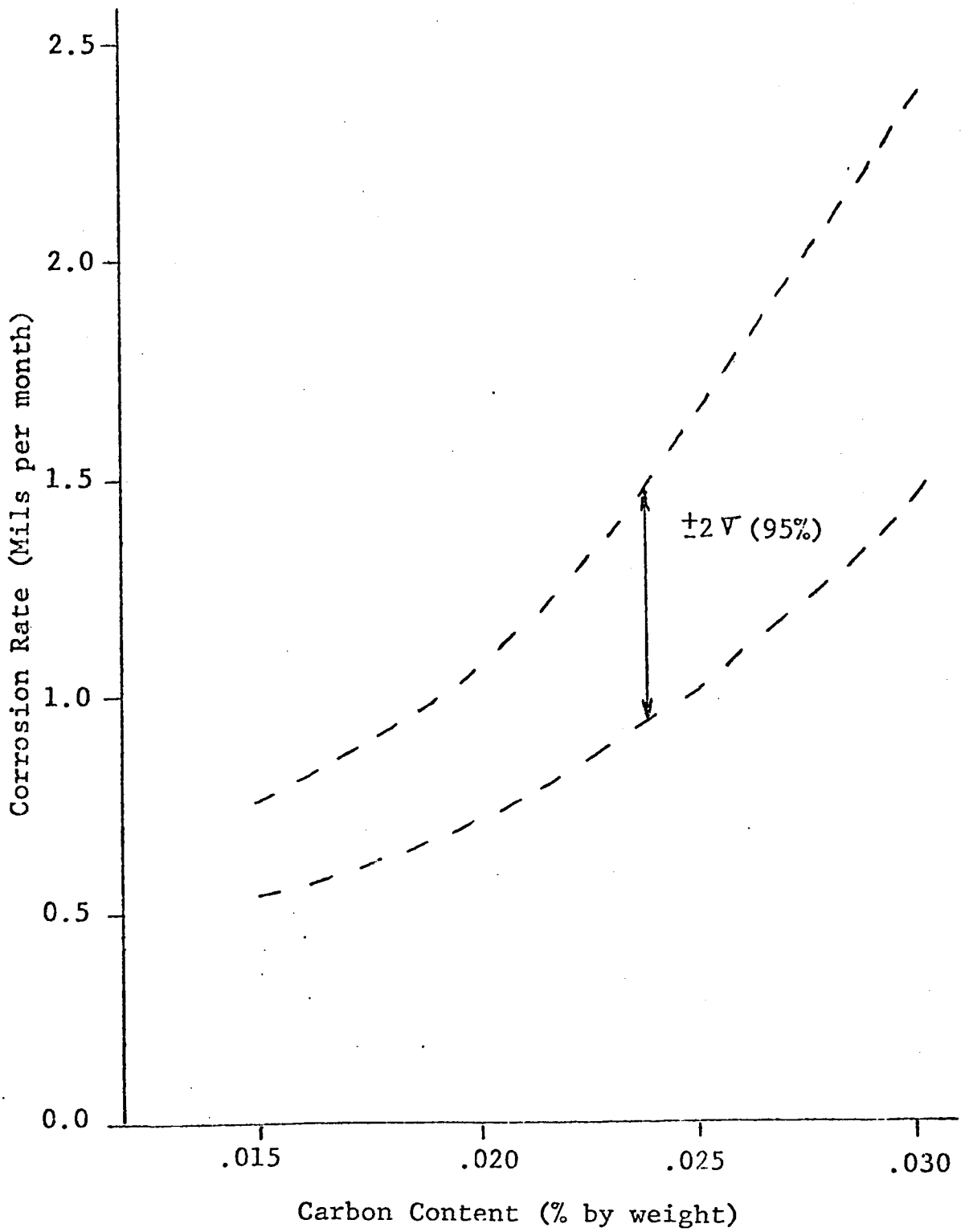

Figure 8. Carbon content versus corrosion rate.

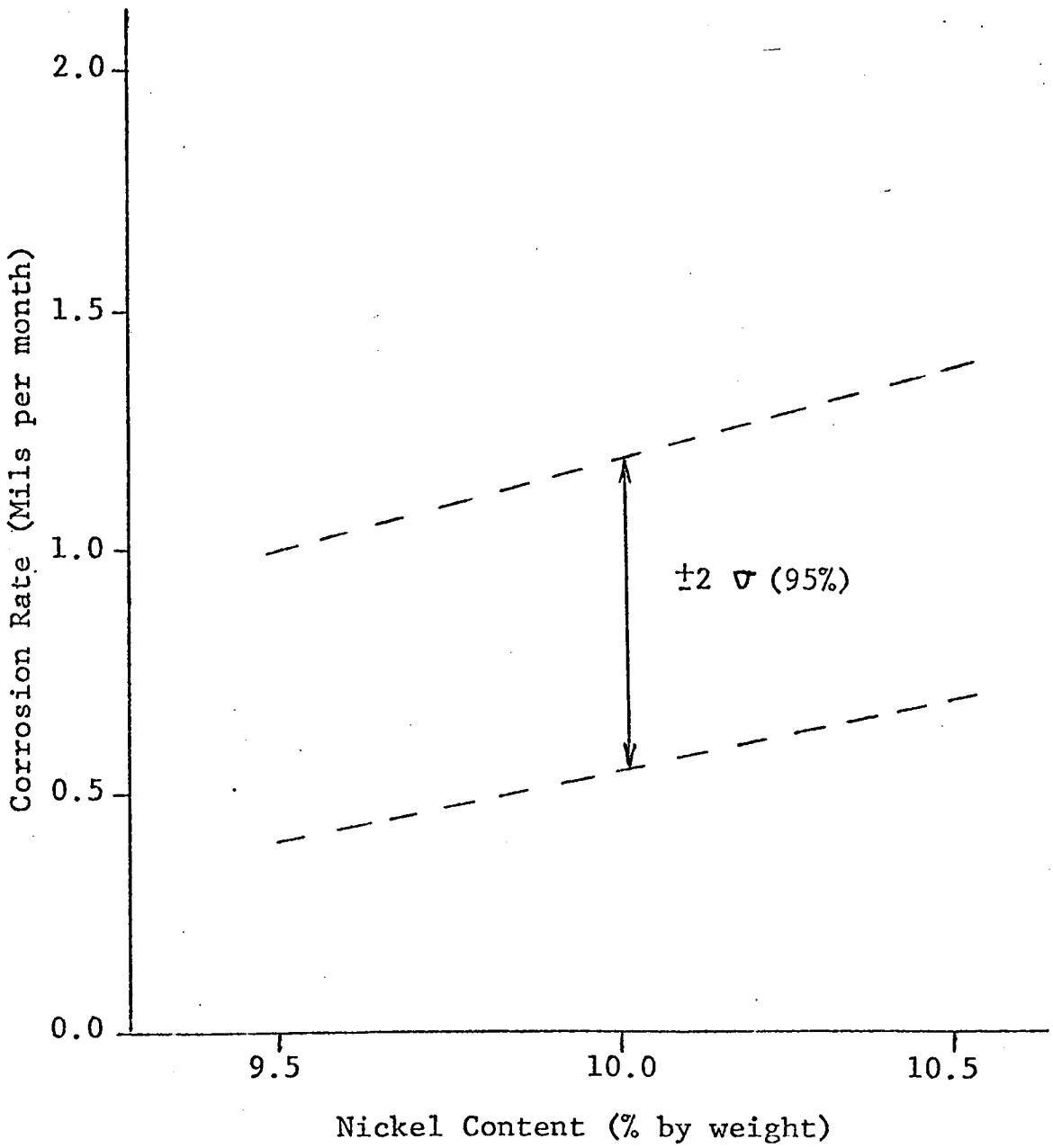

Figure 9. Nickel content versus corrosion rate.

The corrosion rate in nitric acid versus the manganese concentration is shown in Figure 10. A typical "shotgun" distribution is seen and no systematic variation is noticeable. The manganese concentration was only varied from 1.4% to 1.7% with all other elements remaining constant. However, these limited results compare favorably with historical data which show that manganese has no effect over this range of concentrations.

Silicon, although tested from contents ranging from 0.35% to 0.65%, showed no significant effect on the corrosion rate of TP-304-L in the nitric acid test (see Figure 11). Almost all commercial heats of TP-304-L would have silicon contents within this range, as the maximum allowable silicon content is 0.75%.

Sulfur and phosphorous were not evaluated due to the lack of spread in the concentrations of both elements, while holding all other elements constant. The conclusion of this report is that if these two elements are held respectively within the midrange of allowable concentrations that they have no significant effect on the corrosion rate of TP-304-L in nitric acid.

Molybdenum concentrations below 0.15% had no effect on the corrosion rate of TP-304-L in the nitric acid test. Molybdenum only becomes a significant modifier when the ferrite phase is present. This will be discussed at length later in this paper.

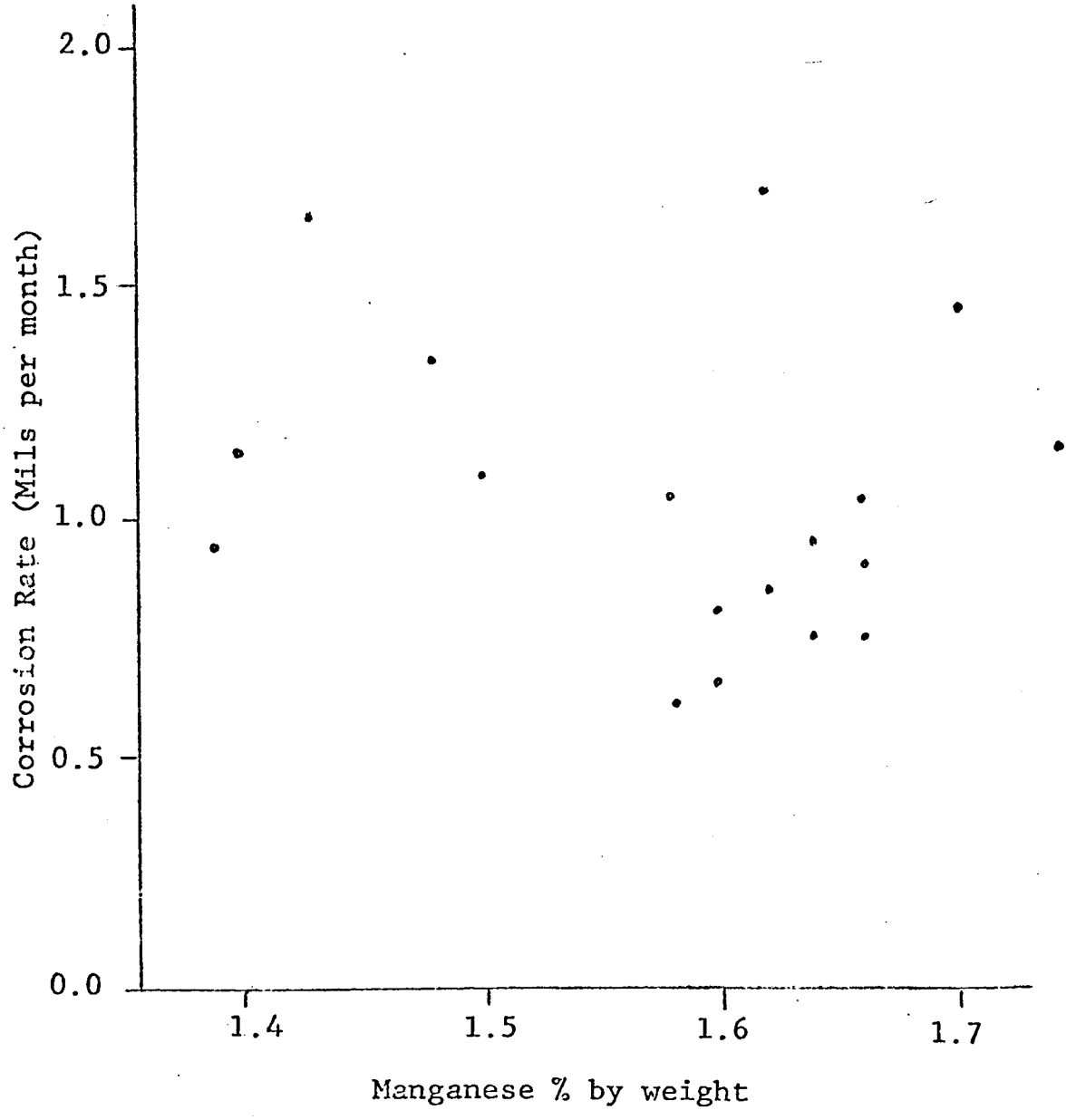

Figure 10. Manganese content versus corrosion rate.

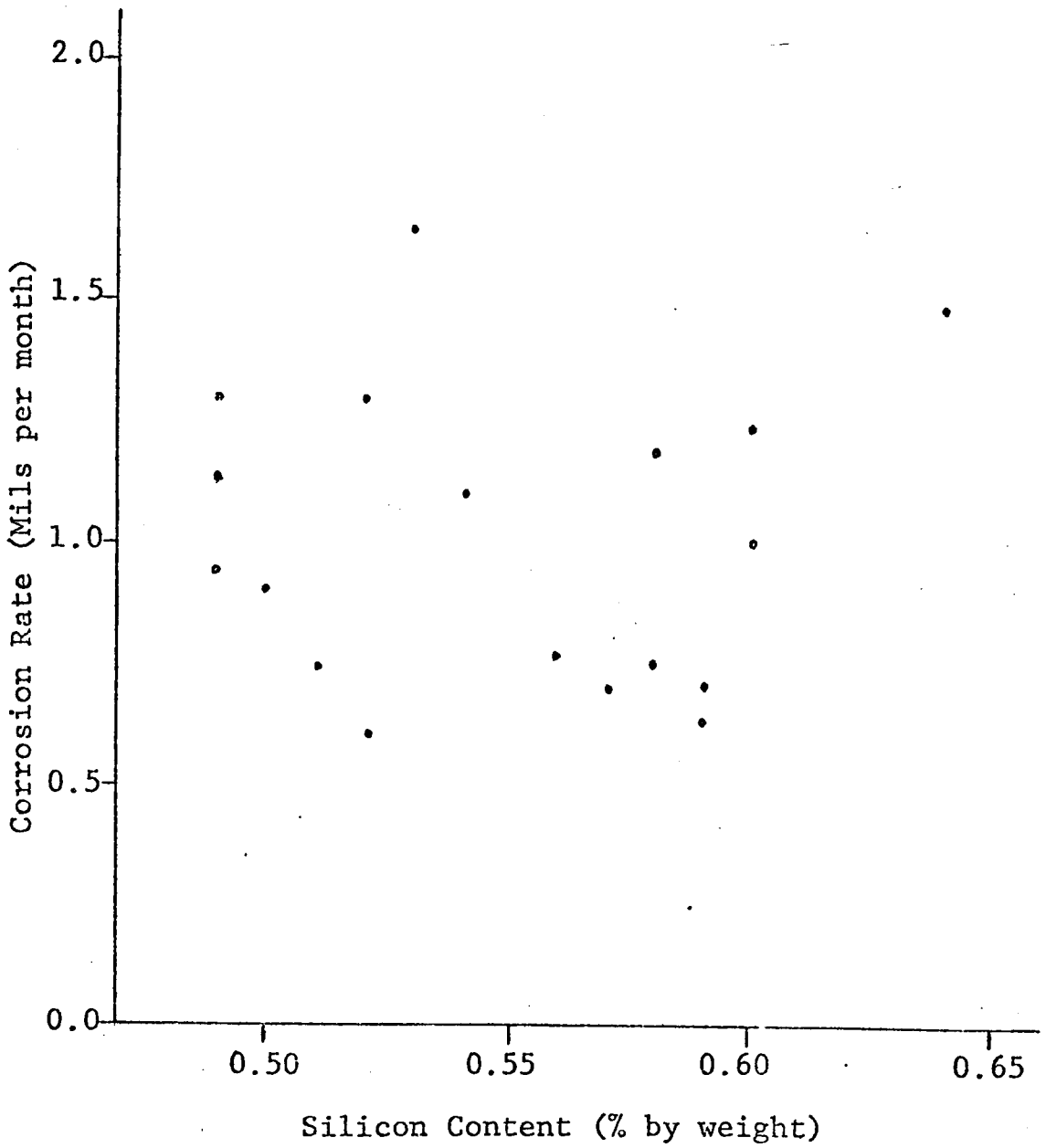

Figure 11. Silicon content versus corrosion rate.

Nitrogen contents were held constant at 0.035% ± .005% during all tests. The nitrogen content remained relatively constant in all test samples and was therefore not significantly varied to show any effect. Historically, this 0.035% concentration of nitrogen has no effect on the corrosion rate of TP-304-L in the nitric acid test[1].

The chromium concentration had a significant effect on the corrosion rate of TP-304-L in the nitric acid test (see Figure 12). The chromium content was varied from 18.0 to 19.4%. This wide range of chromium concentrations readily showed that as the chromium content increased the corrosion rate steadily decreased. This is expected from historical data and electrochemical data on the effect of chromium in austenitic stainless steels when tested in nitric acid. Wider fluctuations were noted in the two sigma data spread in the lower concentrations of chromium. As the chromium concentration approaches 18.75%, the corrosion rate is lowered, the rate of decreasing corrosion rate levels off and the two sigma spread in results narrows.

B. Effect of Ferrite

The effect of small amounts of residual ferrite was the most significant correlation found. The slight increase in the chromium content with the remainder of the chemical analyses of the elements remaining close to the "base" composition resulted in small increasing percentages of

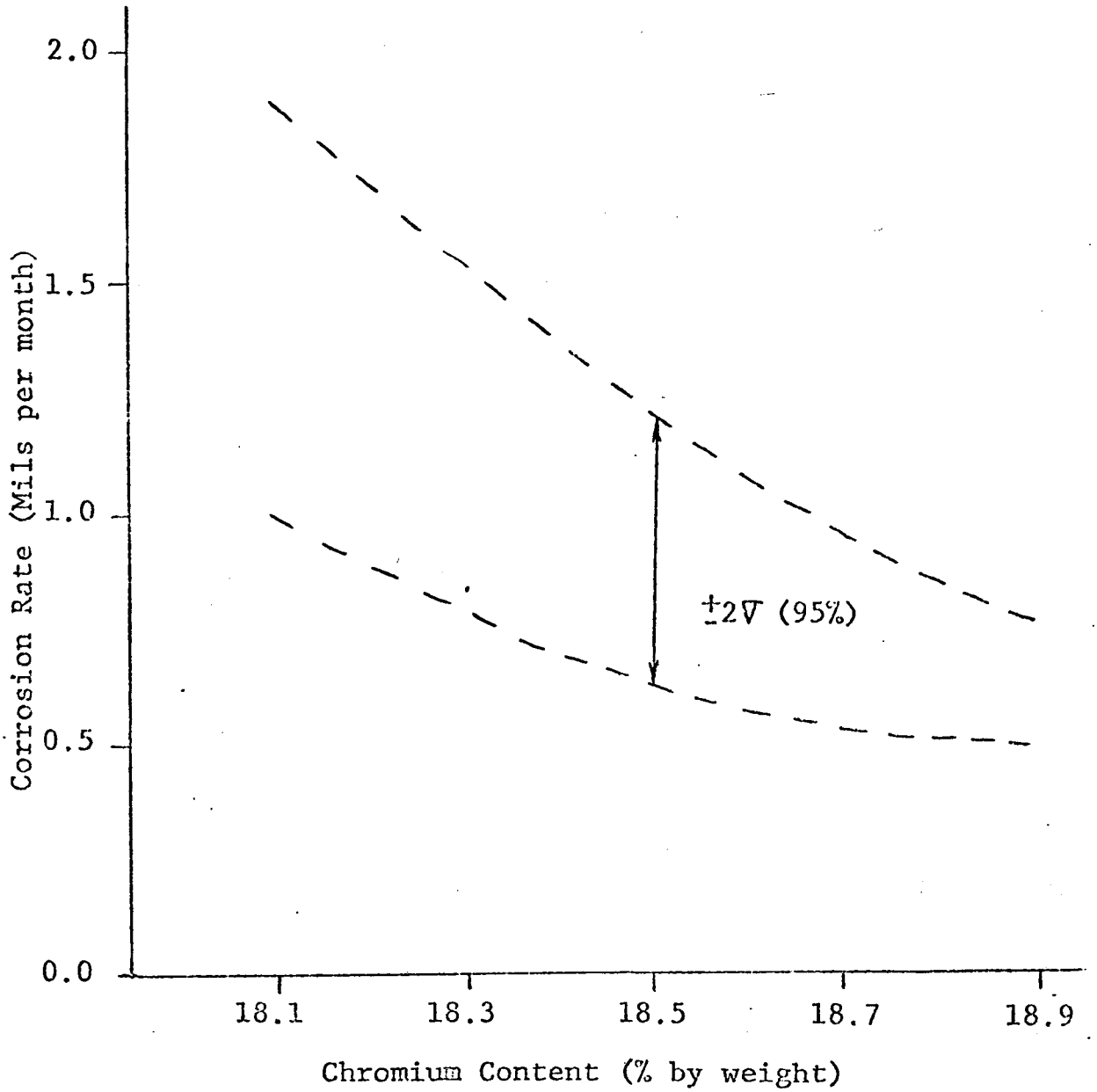

Figure 12. Chromium content versus corrosion rate.

ferrite remaining in some of the test samples after processing and final heat treatment were finished. Table V shows the different chromium and nickel levels between the austenitic matric and the ferrite particles of two heats of TP-304-L.

TABLE V

AUSTENITE AND FERRITE NICKEL AND CHROMIUM CONTENTS

Austenite		Ferrite	
Ni	Cr	Ni	Cr
10.4	18.9	4.8	26.0
10.3	18.6	4.5	24.5

For the ferrite content analysis the carbon concentration was maintained at 0.020% $\pm$ .003%. This was done to eliminate this potent variable from distorting the results.

The ferrite contents versus corrosion rate are shown in Figure 13. The ferrite values shown in this figure were calculated from the American Welding Society Data Sheet reproduced in Figure 14[19].

This is a graphical representation of the amount of ferrite present when the relative amounts of ferrite and

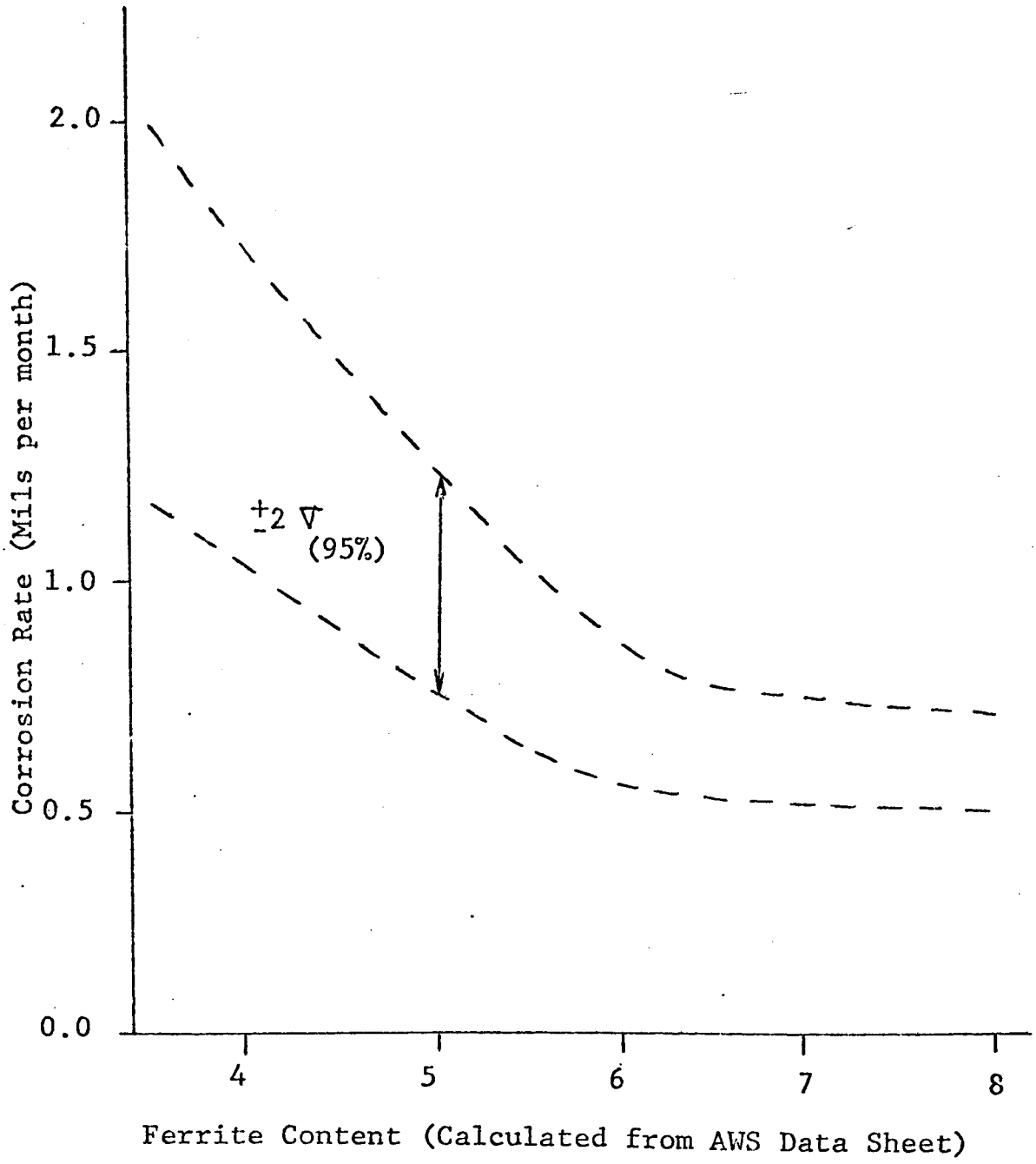

Figure 13. Ferrite (as cast) versus corrosion rate.

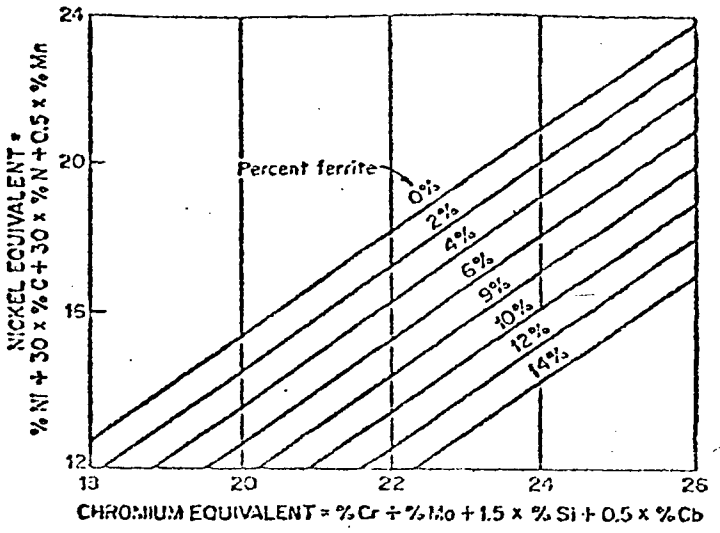

Figure 14. American Welding Society data sheet for calculation of ferrite.[12]

factors for several elements is presented in Table VI.

TABLE VI

FERRITE AND AUSTENITE FORMERS

Ferrite Former	Multiplier	Austenite Former	Multiplier
Chromium	1.0	Nickel	1.0
Silicon	1.5	Manganese	0.5
Molybdenum	1.0	Carbon	30
Columbium	0.5	Nitrogen	30

It should be emphasized that Figure 14 is a correlation to weld deposited material. In producing tubular products, the ferrite in the as-cast billets and final wrought product

is of interest. The ferrite content metallographically observed in cast TP-304-L was generally 2% points higher than calculated from Figure 12 for weld deposited material.

Also, the calculated percent ferrite values were observed to be 5 to 6% points above the percent ferrite observed in final size wrought tubular TP-304-L products. This is due to the unstable condition of the ferrite. As the ferrite phase is heat treated above 1950°F the amount of ferrite decreases with time at these high temperatures.

The corrosion rate levels off at 0.7 mils per month when ferrite remains in the as-tested specimens. The corrosion rate increases with the absence of ferrite. This would be due to the effect of chromium content and nickel content. Again the carbon content was held at 0.020% $\pm$ .002% for all these test samples. Photomicrographs support these observations. Figures 15 and 16 show the intergranular corrosion effects of the residual ferrite--almost no intergranular corrosion is present. The corrosion has been reduced to general corrosion of the TP-304-L. Figures 17 and 18 show the intergranular corrosion effects of a lack of residual ferrite.

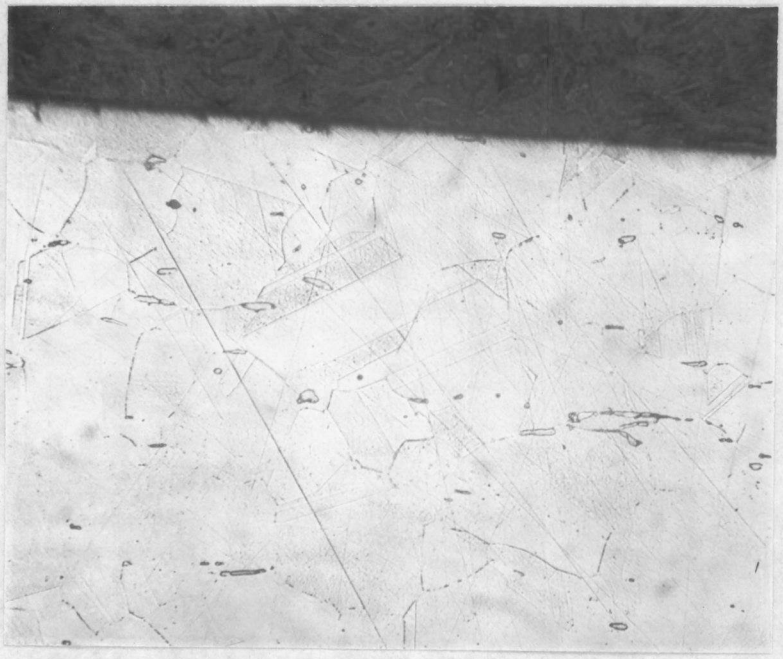

Figure 15. Photomicrograph of Heat LSM9H. Longitudinal Sample - 200X - Oxalic Etch.

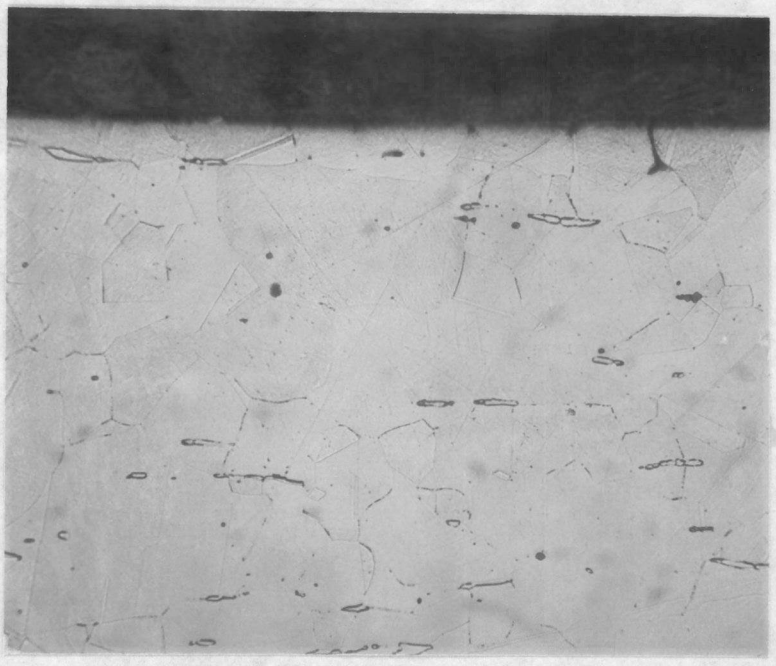

Figure 16. Photomicrograph of Heat LSM8N. Longitudinal Sample - 200X - Oxalic Etch.

Figure 17. Photomicrograph of Heat LWH7T. Longitudinal Sample - 200X - Oxalic Etch.

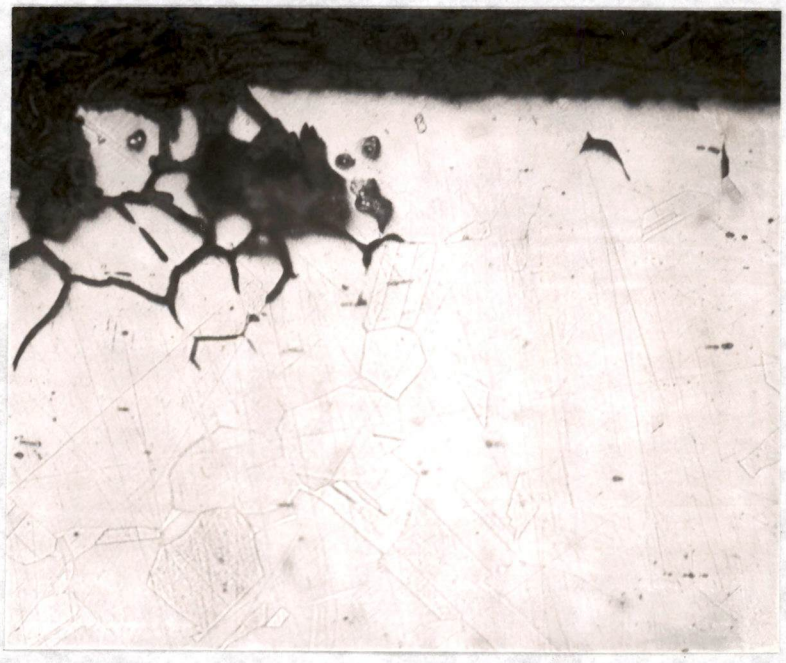

Figure 18. Photomicrograph of Heat LWG31V. Longitudinal Sample - 200X - Oxalic Etch.

C. Ferrite-Molybdenum Interaction

Low concentrations of molybdenum, 0.15% or less, were shown to have no effect on the corrosion rate of TP-304-L in the nitric acid test. However, if the ferrite phase was present and the molybdenum content was over 0.25% a detrimental effect on the corrosion rate was observed (see Figure 19). The ferrite contents were between two and three and carbon was 0.02% to keep the effect of these variables to a minimum to study the effects of molybdenum.

During the test results the higher ferrite test samples with molybdenum contents over 0.25% had a different pattern to the corrosion rates during the five periods when compared to all the other test results. An initial increase in corrosion rate which slowed in later test periods (see Figure 20) was observed.

The corrosive attack in this particular case was the preferential dissolution of the ferrite phases instead of the normally expected intergranular attack (see Figure 21). This photomicrograph shows the corrosive attack to be in the ferrite-austenite boundary regions. Molybdenum, a strong ferrite former, is known to segregate in the ferrite phase. Why this phenomenon occurs will have the attention of future work.

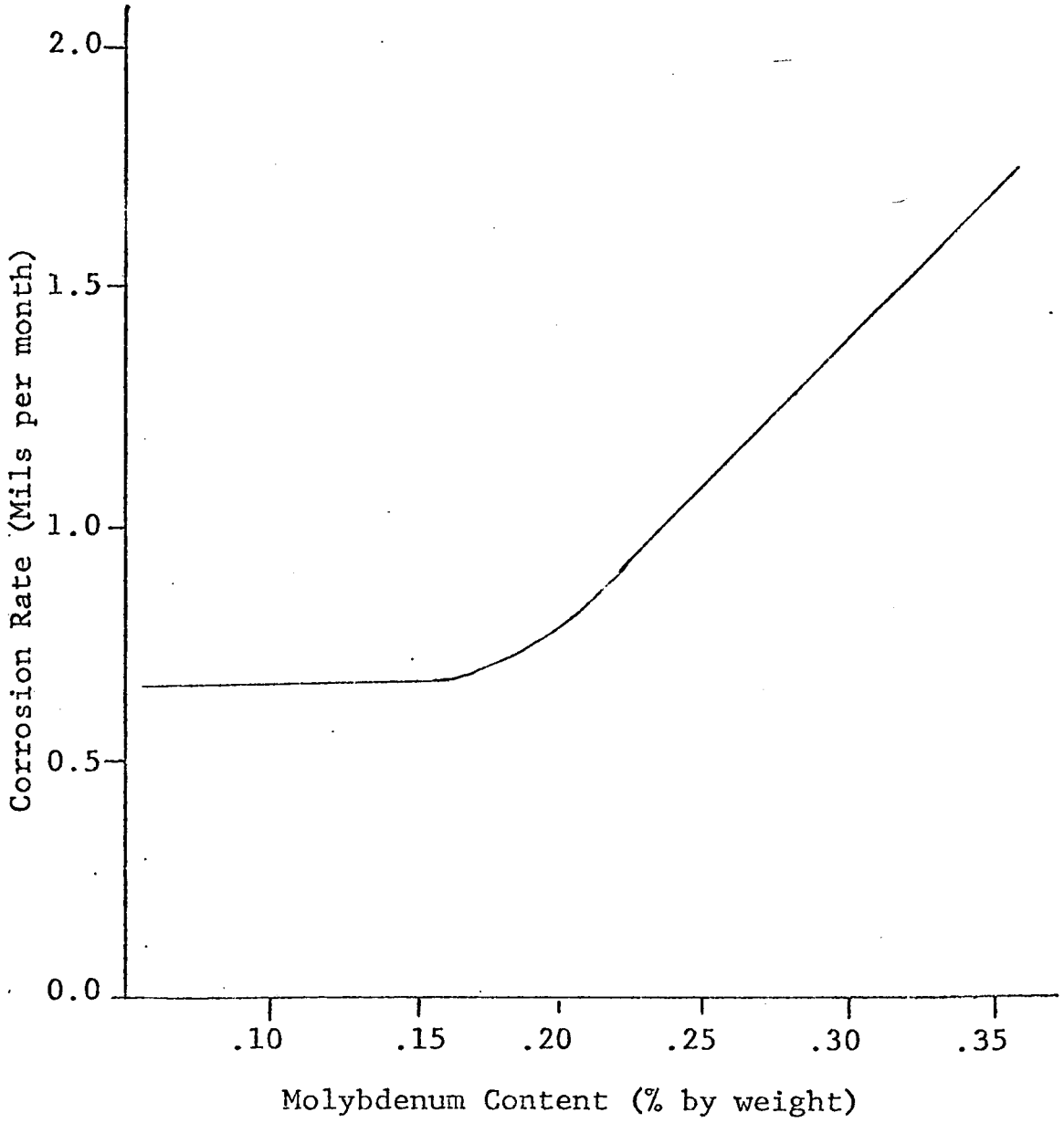

Figure 19. Molybdenum content with constant ferrite versus corrosion rate.

NOTE: Observed ferrite of samples was 1 to 3% as tested.

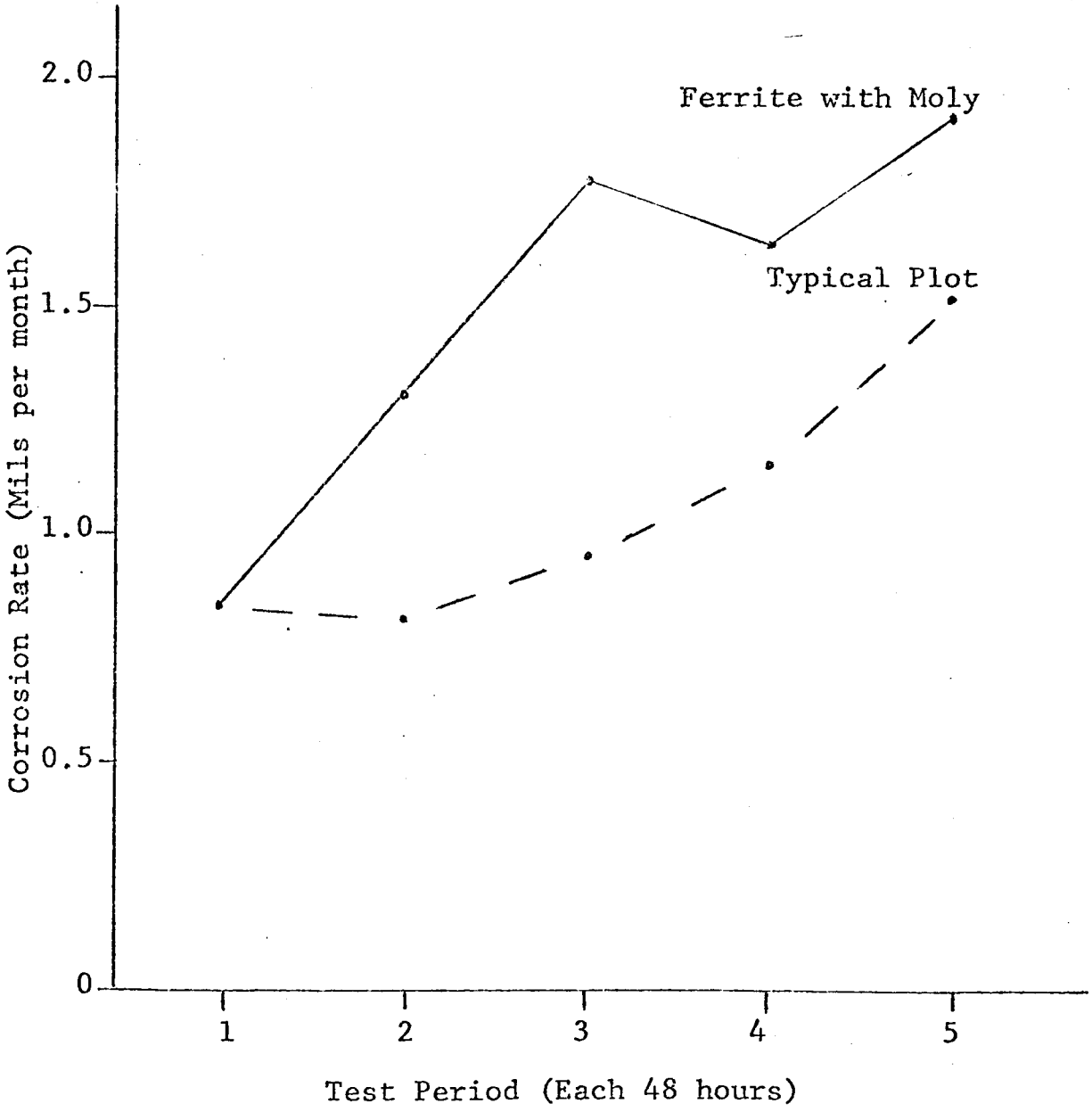

Figure 20. Typical plot of the five test periods of the Nitric Acid Test versus plot of molybdenum plus ferrite.

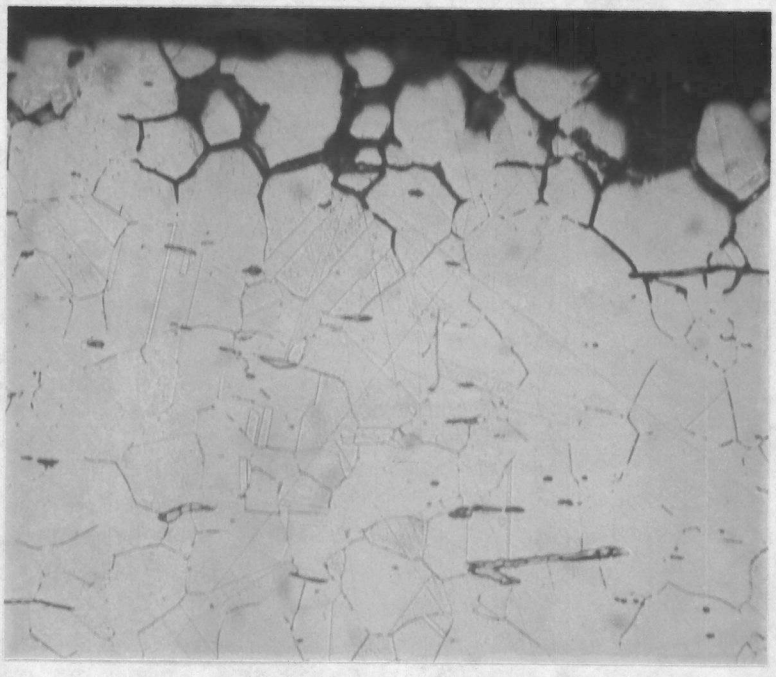

Figure 21. Photomicrograph of Heat LZF8A. Longitudinal Sample - 200X - Oxalic Etch.

Although the corrosion rates were generally higher with the molybdenum plus ferrite situation, the in-service condition would be tolerable. The attack is not intergranular; only the surface ferrite-austenite grain boundaries are dissolved leaving the remainder of the matrix unattacked.

D. Ferrite-Chromium Interaction

To determine whether the ferrite content effect is truly independent or dependent on the chromium content a data matrix comparing chromium and ferrite concentrations was developed. The ferrite values were both the calculated and observed values in the finished TP-304-L tubular product. Table VII shows that the ferrite effect is significantly independent of chromium concentration. At 18.5% chromium, as the residual ferrite remains present the corrosion rate is diminished to 0.7 mils per month and is relatively constant for all chromium levels tested.

E. Conclusions

1. Molybdenum contents higher than 0.25% in TP-304 steel containing small amounts of ferrite decrease the corrosion resistance as measured by the ASTM A-262 Practice C Nitric Acid Test.

2. Small amounts of ferrite in normal TP-304-H steel enhance the corrosion resistance as measured by the ASTM A-262 Practice C Nitric Acid Test.

TABLE VII

CHROMIUM CONTENT AND FERRITE CONTENT
VERSUS CORROSION RATE

Chromium Content (% by weight)	4 Ferrite Content (As Cast) Calculated 0 Ferrite Content (At Final Size) Observed	6 1	8 3
18.8	----	0.7 mils/month	0.6 mils/month
18.5	1.4 mils/month	0.7 mils/month	0.7 mils/month
18.2	1.4 mils/month	0.9 mils/month	----

3. Within the range of composition studied, the response in the Nitric Acid Test relates well to historical data.

LIST OF REFERENCES

LIST OF REFERENCES

1. Binder, W. O., C. M. Brown and R. Franks. "Resistance to Sensitization of Austenitic Chromium - Nickel Steels of 0.03% Maximum Carbon Content." Transactions of the A.S.M. Vol. 41. Metals Park: American Society for Metals, 1949.

2. Gillett, H. W. "Present Knowledge of Low Carbon 18-8." ASTM STP-93. Philadelphia: American Society for Testing and Materials, 1949.

3. Buck, D. C., J. J. Heger, F. J. Phillips and B. R. Queneau. "Corrosion Resistance and Mechanical Properties of Low Carbon Austenitic Stainless Steels." ASTM STP-93. Philadelphia: American Society for Testing and Materials, 1949.

4. American Society for Metals Databook. Metals Park: American Society for Metals, 1977.

5. ASTM A-312-77. Philadelphia: American Society for Testing and Materials.

6. Brown, M. H., W. B. DeLong and W. R. Myers. "An Appraisal of Methods for Evaluating the Corrosion Resistance of Stainless Steels." ASTM STP-93. Philadelphia: American Society for Testing and Materials, 1949.

7. Armijo, J. S. "Intergranular Corrosion of Nonsensitized Austenitic Stainless Steels." Corrosion. Houston: National Association of Corrosion Engineers, 1968.

8. Scharfstein, L. R. "Effects of Residual Elements on the General Corrosion Resistance of Austenitic Stainless Steels." ASTM STP-418. Philadelphia: American Society for Testing and Materials, 1967.

9. Henthorne, M. "Intergranular Corrosion in Iron and Nickel Base Alloys." ASTM STP-516. Philadelphia: American Society for Testing and Materials, 1972.

10. Cowan, R. L. II and C. S. Tedmon, Jr. "Intergranular Corrosion of Iron-Nickel Chromium Alloys." Advances in Corrosion Science and Technology. Volume 3. New York: Plenum Press, 1973.

11. Brown, M. H. "Behavior of Austenitic Stainless Steels in Evaluation Tests for the Detection of Susceptibility to Intergranular Corrosion." Corrosion. Volume 30, No. 1. Houston: National Association of Corrosion Engineers, 1974.

12. Peckner, D. and I. M. Bernstein. Handbook of Stainless Steels. New York: McGraw-Hill, 1977.

13. Fontana, Mars G. and Norbert D. Greene. Corrosion Engineering. New York: McGraw-Hill, 1967.

14. ASTM A-262-70. "Standard Recommended Practices for Detecting Susceptibility to Intergranular Attack in Stainless Steels." Volume 3. Philadelphia: American Society for Testing and Materials, 1975.

15. Streicher, M. A. "Intergranular Corrosion of Stainless Alloys." ASTM STP-656. Philadelphia: American Society for Testing and Materials, 1978.

16. Kohl, et al. "Suitability of the Huey Test for Inspection Purposes." Material Performance. Houston: National Association of Corrosion Engineers, 1974.

17. DuPont, Applied Technology Division. Strategy of Experimentation. Wilmington: DuPont, 1975.

18. McClean, R. A. and V. L. Anderson. Design of Experiments. New York: Marcel Dekker, Inc., 1974.

APPENDIX

TABLE VIII

HEAT ANALYSES SELECTED FOR THE STUDY OF THE EFFECT OF CARBON CONTENT

Heat	Composition, Percent By Weight								Corrosion Rate (Mils Per Month)
	Mn	Cr	Ni	Mo	Si	S	P	C	
LSL11C	1.65	18.35	10.08	.10	.56	.013	.018	.018	0.7
LSM8S	1.60	18.45	9.83	.12	.58	.012	.017	.016	0.7
LSM8V	1.60	18.58	9.78	.12	.52	.014	.018	.016	0.6
LTE23S	1.62	18.35	9.85	.11	.51	.013	.018	.018	0.7
LSL11C	1.65	18.35	10.08	.10	.56	.012	.014	.018	0.7
LSM8S	1.60	18.45	9.83	.12	.58	.012	.017	.016	0.6
LTK5K	1.66	18.43	10.28	.10	.54	.011	.017	.020	0.9
LTE25A	1.55	18.05	10.15	.10	.55	.014	.018	.025	1.1
LTK20T	1.70	18.35	10.23	.10	.53	.012	.013	.021	1.1
LXA30K	1.56	18.58	10.15	.14	.46	.015	.018	.022	1.4
LXA30L	1.35	18.30	9.98	.10	.45	.013	.018	.020	1.0
LXA31A	1.48	18.28	10.15	.12	.48	.014	.021	.020	1.0
LSM9L	1.66	18.63	9.88	.12	.59	.015	.016	.020	1.0
LVM22B	1.40	18.15	10.23	.10	.49	.017	.020	.023	1.4
LVM22N	1.48	18.58	10.08	.10	.52	.015	.019	.022	1.4
LWH7T	1.40	18.10	10.00	.09	.53	.012	.019	.028	1.7
LTM3G	1.69	18.20	9.80	.10	.46	.011	.019	.023	1.7
LWG31V	1.54	18.35	10.20	.11	.52	.013	.020	.027	2.4

TABLE IX

HEAT ANALYSES SELECTED FOR THE STUDY OF THE EFFECT OF THE NICKEL CONTENT

Heat	Composition, Percent By Weight								Corrosion Rate (Mils Per Month)
	Mn	Cr	Ni	Mo	Si	S	P	C	
LSM9G	1.63	18.45	9.78	.12	.57	.013	.017	.022	0.7
LSM9N	1.51	18.23	9.78	.12	.53	.015	.015	.019	0.6
LSM8S	1.60	18.45	9.83	.12	.58	.012	.017	.017	0.7
LTE23S	1.62	18.35	9.85	.11	.51	.013	.018	.018	0.7
LSL11C	1.65	18.35	10.08	.10	.56	.012	.014	.018	0.7
LSM8S	1.60	18.45	9.83	.12	.58	.012	.017	.017	0.6
LTK5K	1.66	18.43	10.28	.10	.54	.011	.017	.020	0.9
LTK20N	1.57	18.33	10.18	.10	.53	.014	.013	.019	1.0
LTE24C	1.57	18.35	10.33	.10	.47	.012	.013	.023	0.8
LXA31F	1.63	18.45	9.95	.13	.50	.013	.018	.022	0.9
LSM9L	1.66	18.63	9.88	.12	.59	.015	.016	.020	1.0
LWNN3A	1.60	18.53	10.38	.10	.56	.012	.019	.020	1.3
LVN5V	1.38	18.30	10.43	.10	.53	.016	.018	.017	1.2
LWF6XS	1.48	18.48	10.38	.11	.48	.011	.016	.021	1.1
LVL24W	1.51	18.51	10.50	.10	.48	.020	.018	.023	1.2
LTE25G	1.72	18.45	10.10	.10	.54	.011	.013	.023	1.1
LSM9G	1.63	18.45	9.78	.12	.57	.013	.017	.022	0.7
LNV13K	1.45	18.15	10.63	.10	.44	.015	.018	.019	1.2

TABLE X

HEAT ANALYSES SELECTED FOR THE STUDY OF THE EFFECT OF MANGANESE

Heat	Composition, Percent By Weight								Corrosion Rate (Mils Per Month)
	Mn	Cr	Ni	Mo	Si	S	P	C	
LSM9G	1.63	18.45	9.78	.12	.57	.013	.017	.022	0.7
LSM8S	1.60	18.45	9.83	.12	.58	.012	.017	.017	0.6
LSM8V	1.60	18.58	9.78	.12	.52	.014	.018	.023	0.6
LTE235	1.62	18.35	9.85	.11	.51	.013	.018	.018	0.7
LSL11C	1.65	18.35	10.08	.10	.56	.013	.016	.021	0.7
LSM8S	1.60	18.45	9.83	.12	.58	.012	.017	.017	0.6
LTK20N	1.57	18.33	10.18	.10	.53	.014	.013	.019	1.1
LSM9G	1.63	18.45	9.78	.12	.57	.013	.017	.022	0.7
LTE24C	1.35	18.35	10.23	.10	.47	.012	.013	.023	1.0
LXA31F	1.63	18.45	9.95	.13	.50	.013	.018	.022	0.9
LSM9L	1.66	18.63	9.88	.12	.59	.015	.016	.020	1.0
LVN5V	1.59	18.30	10.13	.10	.53	.016	.018	.017	1.2
LVM22N	1.48	18.58	10.08	.10	.52	.015	.019	.022	1.4
LTM3G	1.69	18.20	9.80	.10	.46	.011	.019	.023	1.7
LSM10N	1.67	18.30	9.98	.11	.59	.016	.016	.018	1.2
LXB15A	1.55	18.43	10.28	.10	.45	.017	.018	.022	1.5
LWF6C	1.40	18.30	9.85	.10	.49	.014	.015	.021	1.1
LTE25G	1.72	18.45	10.10	.10	.54	.011	.013	.023	1.1
LTE2YK	1.58	18.65	10.10	.10	.51	.010	.013	.022	0.6

TABLE XI

HEAT ANALYSES SELECTED FOR THE STUDY OF THE EFFECT OF THE SILICON CONTENT

Heat	Composition, Percent By Weight								Corrosion Rate (Mils Per Month)
	Mn	Cr	Ni	Mo	Si	S	P	C	
LSM9G	1.63	18.45	9.78	.12	.57	.013	.017	.022	0.7
LSM8E	1.66	18.35	9.88	.12	.58	.015	.017	.017	0.6
LSM8S	1.60	18.45	9.83	.12	.58	.012	.017	.017	0.7
LTE23S	1.62	18.35	9.85	.11	.51	.013	.018	.018	0.7
LSL11C	1.65	18.35	10.08	.10	.56	.012	.014	.018	0.7
LSM8H	1.62	18.73	9.95	.12	.58	.014	.022	.022	0.6
LSM9G	1.63	18.45	9.78	.12	.57	.013	.017	.022	0.7
LVM22N	1.48	18.58	10.08	.10	.52	.015	.019	.022	1.4
LTK27C	1.61	18.05	9.95	.10	.45	.012	.011	.017	1.0
LXA31F	1.63	18.45	9.95	.13	.50	.013	.018	.022	0.9
LSM9L	1.66	18.63	9.88	.12	.59	.015	.016	.020	1.0
LSM8A	1.58	18.53	9.75	.12	.57	.012	.021	.020	1.2
LVM13G	1.45	18.43	9.83	.12	.51	.016	.020	.023	1.4
LTM3G	1.69	18.20	9.80	.10	.53	.011	.019	.017	1.7
LSM10M	1.64	18.43	9.80	.12	.59	.015	.015	.020	1.2
LWB12Z	1.42	18.18	10.13	.12	.63	.012	.018	.019	1.5
LVM21M	1.53	18.55	10.28	.11	.49	.015	.022	.019	1.1
LTE25G	1.72	18.45	10.10	.10	.54	.011	.013	.023	1.1

TABLE XII

HEAT ANALYSES SELECTED FOR THE STUDY OF THE EFFECT OF THE CHROMIUM CONTENT

Heat	Composition, Percent By Weight								Corrosion Rate (Mils Per Month)
	Mn	Cr	Ni	Mo	Si	P	S	C	
LSM9K	1.67	18.78	10.05	.12	.61	.017	.015	.022	0.6
LSM8N	1.70	18.93	9.90	.12	.56	.014	.023	.021	0.6
LSL11C	1.65	18.35	10.08	.10	.56	.012	.014	.018	0.7
LSM8V	1.60	18.58	9.78	.12	.52	.014	.018	.020	0.6
LSM8S	1.60	18.45	9.83	.12	.58	.012	.017	.017	0.7
LSM8E	1.66	18.85	9.88	.12	.58	.015	.017	.018	0.6
LSM8N	1.70	18.93	9.90	.12	.56	.014	.023	.021	0.6
LTE23S	1.62	18.35	9.85	.11	.51	.013	.018	.018	0.7
LSM7W	1.56	18.75	9.85	.12	.59	.013	.019	.023	0.9
LSM8H	1.62	18.73	9.95	.12	.58	.014	.022	.022	0.6
LSL11C	1.65	18.35	10.08	.10	.56	.012	.014	.018	0.7
LSM8S	1.60	18.45	9.83	.12	.58	.012	.017	.017	0.6
LTK27K	1.73	18.05	10.05	.10	.52	.010	.013	.020	1.0
LTE25A	1.55	18.05	10.15	.10	.51	.011	.014	.024	1.1
LXA30L	1.35	18.30	9.98	.10	.45	.013	.018	.020	1.0
LVL2H	1.58	18.00	10.00	.10	.50	.012	.016	.017	1.2
LVM22K	1.50	18.30	10.05	.14	.46	.013	.021	.022	1.2
LWB12X	1.40	18.15	10.10	.10	.44	.020	.017	.019	1.4
LWH7T	1.40	18.10	10.00	.09	.53	.012	.019	.023	1.7
LSM10N	1.67	18.30	9.98	.11	.59	.016	.016	.018	1.2
LWG31Z	1.48	18.20	10.00	.06	.46	.014	.018	.022	1.8
LWH1A	1.45	18.15	10.10	.05	.51	.014	.018	.020	1.5
LWB27Z	1.63	18.40	10.10	.10	.63	.013	.019	.019	1.5

TABLE XII (Continued)

Heat	Composition, Percent By Weight								Corrosion Rate (Mils Per Month)
	Mn	Cr	Ni	Mo	Si	P	S	C	
LWF6C	1.40	18.30	9.85	.10	.49	.014	.015	.021	1.1
LSM9F	1.69	18.83	10.00	.12	.56	.015	.015	.017	0.9
LSM8B	1.58	18.78	9.85	.12	.56	.013	.017	.023	0.7
LTE25G	1.72	18.45	10.10	.10	.54	.011	.013	.023	1.1
LSM9H	1.59	18.85	9.95	.12	.57	.015	.017	.018	0.6
LTE24K	1.58	18.65	10.10	.10	.51	.010	.013	.022	0.6

TABLE XIII

HEAT ANALYSES SELECTED FOR THE STUDY OF THE CALCULATED FERRITE PHASE PRESENT

Heat	Composition, Percent By Weight									Calculated Ferrite	Corrosion Rate (Mils/Month)
	Mn	Cr	Ni	Mo	Si	S	P	C	N		
LSM8A	1.58	18.53	9.75	.12	.57	.012	.021	.020	.035	7	0.8
LTE25G	1.72	18.45	10.10	.10	.54	.011	.013	.023	.038	4½	1.1
LSM8D	1.68	18.65	9.75	.12	.59	.015	.016	.018	.033	7	0.8
LSM9G	1.63	18.45	9.78	.12	.57	.013	.017	.022	.040	6	0.7
LTE25B	1.73	18.60	10.45	.10	.55	.014	.018	.019	.034	4	1.7
LTE24K	1.58	18.65	10.10	.10	.51	.010	.013	.022	.037	6	0.6
LSM9F	1.69	18.83	10.00	.12	.56	.015	.015	.017	.034	7	0.9
LSM8B	1.58	18.78	9.85	.12	.56	.013	.017	.023	.037	7	0.7
LTE25M	1.80	19.45	10.95	.10	.59	.011	.012	.017	.035	5	1.0
LTE24B	1.61	18.75	10.23	.10	.46	.012	.014	.022	.037	5½	0.6
XWMN2T	1.44	18.53	10.25	.10	.62	.010	.017	.022	.038	4	1.7
LTE2YC	1.57	18.85	10.33	.10	.47	.012	.013	.023	.039	6	0.5
LXA30K	1.56	18.58	10.15	.14	.46	.015	.018	.022	.040	4½	1.4
LXA30L	1.35	18.30	9.98	.09	.45	.013	.018	.020	.035	5	1.0
LXA31A	1.48	18.28	10.15	.12	.48	.014	.021	.020	.036	4½	1.0
LVL2H	1.58	18.00	10.00	.10	.50	.012	.016	.017	.032	3½	1.2
LVM22B	1.40	18.15	10.23	.10	.49	.017	.020	.023	.038	3	1.4
LVM22K	1.50	18.30	10.05	.14	.46	.013	.021	.022	.037	4	1.2
LWF6B	1.44	18.55	10.03	.10	.53	.013	.017	.023	.041	4½	1.7

TABLE XIII (Continued)

Heat	Composition, Percent By Weight									Calculated Ferrite	Corrosion Rate (Mils/Month)
	Mn	Cr	Ni	Mo	Si	S	P	C	N		
LVL24W	1.51	18.51	10.50	.10	.48	.020	.018	.023	.042	3½	1.2
LWH1A	1.45	18.15	10.10	.05	.51	.014	.018	.020	.034	3½	1.5
LWE9L	1.51	18.93	10.98	.10	.47	.014	.015	.020	.037	4	1.1
LWE9K	1.38	18.38	10.60	.10	.44	.014	.015	.021	.035	3½	1.1
LSM9H	1.59	18.85	9.95	.12	.57	.015	.017	.018	.034	8½	0.6
LTE25H	1.69	18.70	10.20	.10	.56	.012	.014	.020	.033	6	0.8
LWB12X	1.40	18.13	10.10	.10	.44	.020	.017	.019	.037	4	1.4
LWE9B	1.42	18.38	10.35	.10	.47	.014	.018	.023	.041	3½	1.8
LSM9K	1.67	18.78	10.05	.12	.61	.017	.015	.022	.040	6½	0.6
LSM8N	1.70	18.93	9.90	.12	.56	.014	.023	.021	.036	8	0.6
LTE25D	1.75	18.70	10.50	.10	.58	.011	.011	.021	.042	5	0.8
LSM9M	1.57	18.43	9.75	.11	.56	.013	.016	.021	.037	6	0.7
LSL11C	1.65	18.35	10.08	.10	.56	.012	.014	.018	.036	5	0.7
LSM8S	1.60	18.45	9.83	.12	.58	.012	.017	.017	.041	6½	0.7
LSM8E	1.66	18.85	9.88	.12	.58	.015	.017	.017	.033	8	0.6
LSM9H	1.59	18.85	9.95	.12	.57	.015	.017	.018	.034	8	0.6
LTE23S	1.62	18.35	9.85	.11	.51	.013	.018	.018	.042	5½	0.7
LSM8H	1.62	18.73	9.95	.12	.58	.014	.022	.022	.038	6½	0.6

TABLE XIV

HEAT ANALYSES SELECTED FOR THE STUDY OF THE EFFECT OF THE CALCULATED FERRITE PLUS MOLYBDENUM PRESENT

Heat	Composition, Percent By Weight									Calculated Ferrite	Corrosion Rate (Mils/Month)
	Mn	Cr	Ni	Mo	Si	S	P	C	N		
L0274	1.53	18.70	10.35	.25	.50	.015	.024	.016	.032	8½	0.9
L0279	1.58	18.75	9.88	.25	.61	.012	.023	.029	.037	9	1.2
LZF18B	1.40	18.53	10.13	.20	.55	.011	.017	.021	.034	8½	0.7
L0281	1.62	19.00	10.10	.40	.63	.012	.025	.026	.035	10	1.8

VITA

William Henry Zielke was born in Milwaukee, Wisconsin on July 13, 1947. He attended grade schools in that city. The Zielke family moved to Chattanooga, Tennessee in 1962. He graduated from Notre Dame High School in June, 1965 and the following September entered The University of Cincinnati. After co-oping with the Atomic Energy Commission plant in Fernald, Ohio, he received a Bachelor of Science Degree in Metallurgical Engineering in June, 1970.

After graduation Mr. Zielke was employed at Combustion Engineering's Metallurgical Research and Development Laboratory in Chattanooga, Tennessee. In the Spring of 1971 he started to attend night classes sponsored by the University of Tennessee at Knoxville. In 1973 he transferred to Combustion Engineering's Tube Manufacturing Plant as the Plant Metallurgist.

He is married to the former Barbara Molleran of Cincinnati, Ohio. They have two sons, Mark and John.